Wideband Dipole Array Loaded Substrate-Integrated Horn Array With Improved Sidelobe Performance

Jingxue Wang, Yujian Li, *Member, IEEE*, and Junhong Wang, *Senior Member, IEEE*

***Abstract*—In this letter, a novel millimeter-wave substrate-integrated *H*-plane horn array is presented by combining a loaded dipole array and the gap substrate-integrated waveguide consisting of eight etched slits. The operating mechanism and design process of the array are investigated. A wide impedance bandwidth of 33%, a gain up to 14.6 dBi, and symmetrical radiation patterns with cross polarizations of less than –23 dB are verified experimentally by a 1 × 4 fabricated prototype. An improved sidelobe level of almost less than –10 dB is also achieved over the wideband even though the element spacing of the array is larger than two operating wavelengths. The proposed method is valuable for the realization of wideband high-gain planar horn arrays with large element spacing, which is an attractive candidate for millimeter-wave applications.**

***Index Terms*—End-fire radiation, millimeter waves, phase correction, sidelobe level, substrate-integrated horn array.**

I. Introduction

WIDEBAND high-gain antenna arrays are highly demanded by millimeter-wave communications in order to compensate the large atmosphere propagation loss and achieve the high data rate. In comparison with the widely used radiating elements, such as the dipole and microstrip patch antennas, a larger radiating aperture can be achieved by the horn element, which would be helpful in reducing the required number of antenna elements for the array design with a fixed physical size and simplifying the geometry of the feed network of the array [1]. However, conventional horn arrays usually suffer from a high sidelobe level due to the element spacing of larger than one operating wavelength. To solve the issue, a dual-mode horn element was designed in [1], and an improved sidelobe level of around -10 dB has been obtained over a bandwidth of 10% by the 4 × 4 horn array. Furthermore, by combining two subarrays with shifted sideways, the 16 × 16 horn array reported in [2] had a low sidelobe level of about –16 dB across a narrow bandwidth of 1.7%.

Beneficial from the advantage of ease of integrating into planar dielectric laminates, the substrate-integrated *H*-plane sectoral horn antenna initially invented in [3] would be an attractive candidate for millimeter-wave communications. Numerous studies have been dedicated to the improvement in the impedance bandwidth of the antenna by loading various types of impedance transformers [4]–[7]. On the other hand, some technologies to enhance the gain of the horn element have been implemented by utilizing the phase corrected structures [8]–[10]. The concept of the complementary source antenna has also been introduced in designing the substrate-integrated horn in our previous work, which achieved a wide bandwidth, stable gain, and radiation patterns with low backlobe [11].

In terms of the substrate-integrated horn arrays, several designs have been investigated in the literature [5], [12], [13]. It is found that horn aperture sizes of less than λ_0 were selected by all the reported horn arrays for preventing the undesirable high sidelobe level. As a result, the advantage of the aperture size of the horn element was sacrificed, although the satisfying sidelobe level can be obtained. Therefore, it can be seen that the design of wideband horn arrays with a large element spacing and promising sidelobe level simultaneously is still a challenging issue that was seldom addressed in previous studies.

To overcome the aforementioned challenge, a wideband substrate-integrated horn antenna is investigated by combining the dipole array loaded horn antenna [11] with the gap substrate-integrated waveguide (SIW) technology [9]. By this mean, wider bandwidth and better radiating characteristics can be obtained at the same time in comparison with the initial works. By adopting the proposed horn antenna as the radiating element, a novel 1 × 4 wideband substrate-integrated horn array with improved sidelobe level performance is successfully designed even though the element spacing is larger than two operating wavelengths. The method studied in this letter provides a new way to realize the wideband high-gain antenna array composed of radiating elements with large sizes, which would be valuable to future millimeter-wave wireless applications.

II. Design of the Horn Array

A. Horn Element

The substrate-integrated horn antenna with a three-layered geometry is illustrated in Fig. 1. The major structure of the horn with a width of D and a length of L is designed in the middle substrate layer. The size of the horn is determined based on the maximum gain principle of the horn provided in [14]. The width of the feeding SIW a is chosen to ensure that the SIW works in the single TE_{10} mode over the operating band. The diameter and period of the vias s and p are selected according to the design guideline of the SIW given in [15] to prevent the undesirable leakage. The antenna in this letter is designed in Ka-band. Rogers 4003 printed circuit board (PCB) laminates with a relative dielectric constant of 3.55, a loss tangent of 0.0027 at 10 GHz and a thickness of 1.524 mm are applied [16].

The dipole array is loaded in two extra substrate layers with a thickness of h_2 and a total length of $l_{e1} + l_{e2}$, which is

Manuscript received December 1, 2018; accepted December 23, 2018. Date of publication January 31, 2019; date of current version March 1, 2019. This work was supported by the National Natural Science Foundation of China under Grant 61671052 and Grant 61822103. *(Corresponding author: Yujian Li.)*

The authors are with the Institute of Lightwave Technology, Beijing Jiaotong University, Beijing 100044, China (e-mail: 15111011@bjtu.edu.cn; liyujian@bjtu.edu.cn; wangjunh@bjtu.edu.cn).

Digital Object Identifier 10.1109/LAWP.2019.2896600

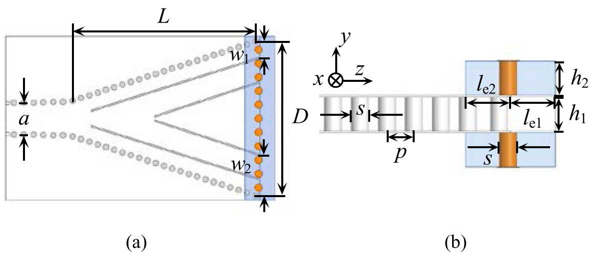

Fig. 1. Geometry of the proposed dipole array loaded substrate-integrated horn antenna with phase corrected structure. (a) Top view. (b) Side view of the horn aperture.

TABLE I
DIMENSIONS OF THE SUBSTRATE-INTEGRATED HORN (UNITS: mm)

Parameters	D	L	a	s	p
Values	20.7	25.5	4.3	0.8	1.3
Parameters	h_1& h_2	l_{e1}	l_{e2}	w_1	w_2
Values	1.524	2	2	2.2	5.45

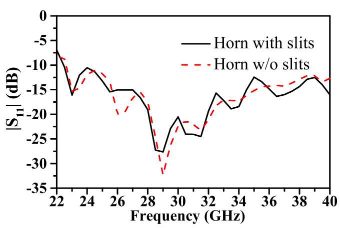

Fig. 2. Simulated $|S_{11}|$ of the horns with and without the slits.

connected to the horn aperture directly. Parameters of h_2, l_{e1}, and l_{e2} are tuned to get good impedance matching performance. It is noted that the selection of the h_2 has to take the available thickness of the substrate into consideration as well. It is found in studies that the impedance matching and radiation properties can improve with the increase of the number of dipoles. However, further improvement is not obvious when the number of dipoles reaches 11. Therefore, an array consisting of 11 dipoles with an element spacing of 1.85 mm is adopted in the design. Moreover, detailed design considerations of the extra substrates and the dipole array can be referred to the previous work in [11]. On the other hand, the gap SIW structure composed of eight slits with a width of 0.2 mm is etched on the top and bottom metallic surface of the horn. The slits are parallel with the sidewalls of the horn. Intervals between the slits and the sidewalls, i.e., w_1 and w_2, are determined based on the cutoff frequency of the gap SIW. The lengths of the slits are tuned to 23.6 and 14.7 mm to get the good phase correction performance. Final values of the geometry parameters are listed in Table I.

The simulated $|S_{11}|$ of the horns with and without the slits are presented in Fig. 2, which demonstrates that the existence of the slits does not affect the impedance matching of the antenna significantly. Beneficial from the merit of the concept of the complementary source horn explored in [11], a wide bandwidth of 56% for $|S_{11}| < -10$ dB (from 22.5 to 40 GHz) that can cover the 28, 27, and 39 GHz bands for the fifth-generation mobile communications is obtained by the design.

In order to investigate the function of the additional slits in this design, simulated electric field distributions at 33 GHz across

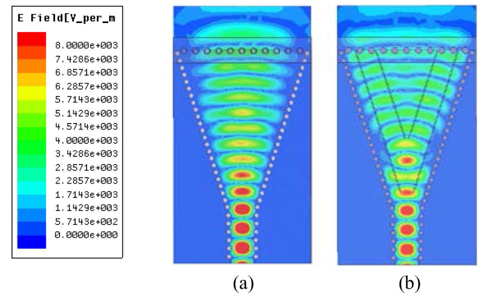

Fig. 3. Simulated electric field distributions at 33 GHz across the horn antennas. (a) Horn without slits. (b) Horn with slits.

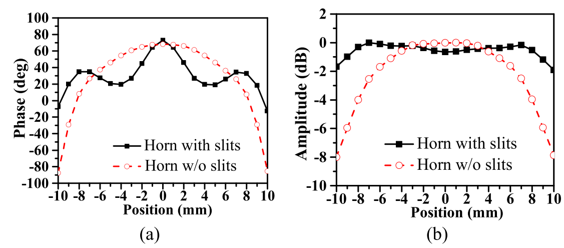

Fig. 4. Simulated electric field distributions over the aperture of the horns with and without the slits at 33 GHz. (a) Phase distribution. (b) Amplitude distribution.

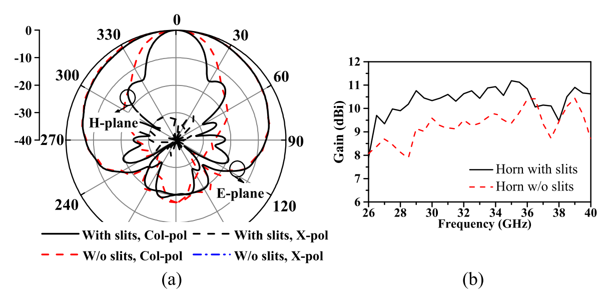

Fig. 5. Simulated radiation performance of the horn antennas with and without the slits at 33 GHz. (a) Radiation pattern. (b) Gain.

the horns with and without the slits are shown in Fig. 3. With the help of the slits, an approximate planar field distribution can be observed in Fig. 3(b). Furthermore, simulated phase and amplitude distributions of the electric field along the horn aperture are plotted in Fig. 4. It is seen that by adding the slits, the phase variation of the field on the aperture is decreased from 155° (varying from –87° to 68°) to 88° (varying from –12° to 76°). As exhibited in Fig. 4(b), a much more stable amplitude distribution can also be achieved. Therefore, it can be confirmed that the gap SIW structure is an effective mean to adjust both the phase and amplitude distributions of the field over the horn aperture.

Fig. 5(a) gives the simulated radiation patterns of the horn antennas with and without the slits at 33 GHz. Comparing with the design without the slits, the field distribution on the aperture is approximately uniform for the horn with the slits and thus a narrowed 3 dB beamwidth in the *H*-plane can be obtained. As the slits only affect the radiation in the *H*-plane, the radiation pattern in the *E*-plane remains almost the same. Besides, the proposed horn has low cross-polarization level and backward radiation as well. A comparison of the simulated gain results

TABLE II
COMPARISON BETWEEN REPORTED AND PROPOSED HORN ANTENNAS

Antennas	Imp. BW (-10 dB)	Gain (dBi)	FTBR (dB)
[9]	20%	7.6-10.9	10
[11]	42%	9.0-11.7	18
This work	56%	9.7-11.2	18

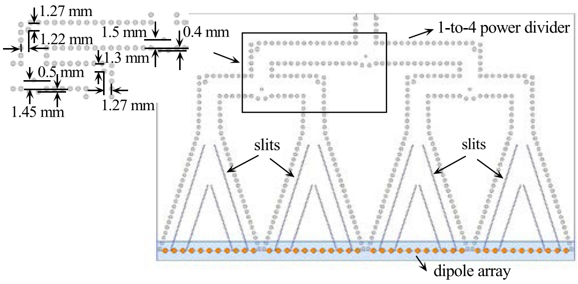

Fig. 6. Geometry of the proposed 1 × 4 horn array with the gap SIW structure.

is presented in Fig. 5(b). The gain of the horn with the slits varies from 9.7 to 11.2 dBi throughout the Ka-band, which is better than the counterpart of the horn without the slits is. Within the frequency range from 26.5 to 36 GHz, a gain enhancement of around 1.5 dB can be achieved by employing the gap SIW structure.

The key characteristics of the proposed antenna are compared with the counterparts of the designs in [9] and [11], as summarized in Table II. It is observed that significant improvement in bandwidth and radiation features can be obtained by this work combining the design methods initially investigated in [9] and [11]. With the help of the loaded dipole array, the proposed horn has much better bandwidth and front to back ratio (FTBR) than those in [9]. Furthermore, although the aperture size and length of this dipole array loaded horn with slits is smaller compared with the horn in [11], the gain of the two designs is still comparable, which is attributed to the almost uniform field distribution over the horn aperture of this letter. Due to the wide operating band and high gain properties, the proposed antenna is desirable for the horn array design in millimeter waves as will be stated in the following part.

B. Horn Array

By employing the proposed radiating element, a 1 × 4 horn array is then designed as illustrated in Fig. 6. A parallel feed network consists of three SIW *T*-junctions is implemented in the Rogers 4003 PCB laminate. Additional inductive vias are placed at the SIW bend and the centerline of the input SIW such to tune the impedance matching. In addition, two vias behind the inductive vias at the centerline are moved in *z*-direction in each *T*-junction to get better impedance matching. Detailed dimensions of the vias are presented in Fig. 6. The simulated bandwidth of the feed network for $|S_{11}| < -10$ dB is 39% (from 27 to 40 GHz) and the insertion loss is around 1.4 dB. Considering the size of the horns, the array has a large element spacing of $2.3\lambda_0$ (λ_0 is the wavelength in free space at 33 GHz). As will be verified in Section III, improved sidelobe and gain performance

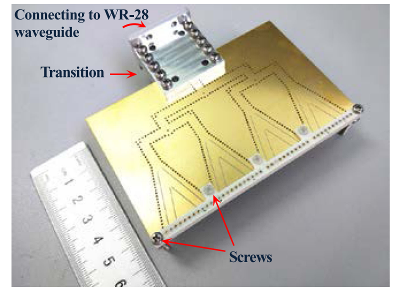

Fig. 7. Photograph of the fabricated prototype of the proposed substrate-integrated *H*-plane horn array with the gap SIW structure.

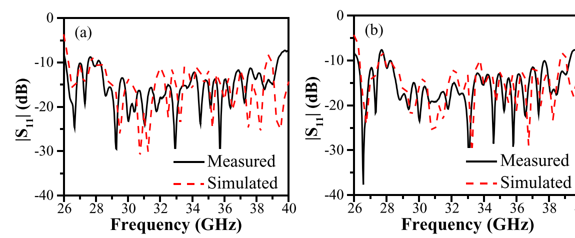

Fig. 8. Measured and simulated $|S_{11}|$ of the horn arrays. (a) With the slits. (b) Without the slits.

can be obtained by the horn array throughout a wide operating band.

III. MEASUREMENT AND DISCUSSION

A prototype of the 1 × 4 horn array was fabricated as exhibited in Fig. 7. A horn array with the same dimensions but without the gap SIW structure was also designed and manufactured for comparison. A wideband SIW to WR-28 waveguide transition initially reported in [17] was integrated at the input port of the horn array for measurement. Three substrate layers of the array were assembled together by using two metallic screws locating at the two ends of the aperture and three plastic screws locating between the horn elements. Conductive glue is added between the adjacent substrate layers to make sure that the dipole array is linked with the horn aperture. An Agilent Network Analyzer E8363C was used for the measurement of $|S_{11}|$. The radiation characteristic of the array was performed in a far-field anechoic chamber. The gain of the arrays was obtained by comparing with a standard horn.

Fig. 8(a) and (b) presents the measured and simulated $|S_{11}|$ of the horn arrays with and without the slits. Good agreement is observed for both designs. The measured impedance bandwidths of horn arrays with and without the slits for $|S_{11}| < -10$ dB are 33% (from 28.2 to 39.3 GHz) and 34% (from 27.8 to 39.3 GHz) respectively, which are close to each other.

Measured and simulated gain results of the two designs are depicted in Fig. 9. The gain of array with the slits varies from 11.9 to 14.6 dBi over the operating band. In the frequency range between 27 and 36 GHz, a gain enhancement of up to 1.3 dB can be achieved by the novel horn array in comparison with the conventional one, which is similar to the improvement of the horn element discussed in Section II-A. A slight difference between the simulation and measurement would be caused by the alignment and measurement tolerances. Besides, the possible uncertainty of the loss feature of the PCB substrates at

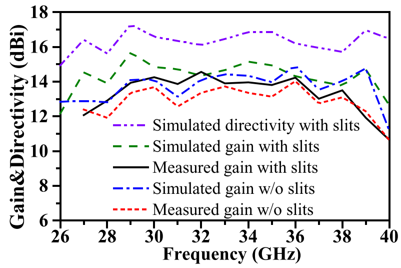

Fig. 9. Measured and simulated gain and simulated directivity of the horn arrays.

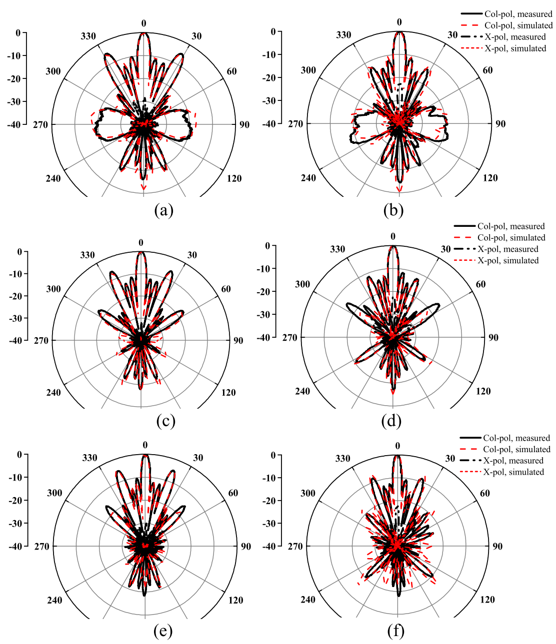

Fig. 10. Measured and simulated radiation patterns of the horn arrays in the H-plane. (a) $f = 28$ GHz, without slits. (b) $f = 28$ GHz, with slits. (c) $f = 33$ GHz, without slits. (d) $f = 33$ GHz, with slits. (e) $f = 38$ GHz, without slits. (f) $f = 38$ GHz, with slits.

millimeter-wave frequencies may also affect the measured results. The simulated directivity of the array with the slits varies from 15.6 to 17.2 dBi in the operating band. The calculated radiation efficiency of the design is around 60%.

Measured and simulated radiation patterns of horn arrays in the H-plane at 28, 33, and 38 GHz are shown in Fig. 10. The radiation patterns of the two arrays are symmetrical and stable over the operating band. Measured cross-polarization level of less than –23 dB and FTBR of larger than 12 dB is obtained. More importantly, significant improvement in the sidelobe feature can be observed by comparing the results of the arrays with and without the slits. To better explore the sidelobe characteristics of the design, Fig. 11 summarizes the measured maximum sidelobe levels of the arrays with and without the slits. The results of the two designs are around –6 dB and almost less than –10 dB, respectively. Specifically, a reduction of about 8 dB in sidelobe level is realized within the frequency range from 28 to 36 GHz, which confirms the advantage of the proposed horn array. A comparison between the reported and the proposed substrate-integrated horn arrays is summarized in Table III. Several types of impedance transformers are applied to the designs in [5], [12]. and [13], but the element spacing is slightly less than λ_0 at the center frequency of the operating band. Different from the designs in the literature, a much larger element spacing of $2.3\lambda_0$ is selected in this letter. Beneficial from the large element spacing, the gain of this array is almost 1 dB higher than those in [5] and [12] are. It is noted that better gain performance would be realized if the substrate with lower dielectric loss is used for the proposed design. Moreover, by introducing the slits to tune the field distribution over the horn aperture, the sidelobe level of this array at the center frequency of the operating band is comparable with the counterparts of the traditional designs with small element spacing. Hence, it is seen that this letter paves a way to overcome the challenge in the design of the planar horn array with large element spacing. On the other hand, the proposed array has a much wider impedance bandwidth as well due to the utilization of the complementary source horn, which is desirable for wideband millimeter-wave applications.

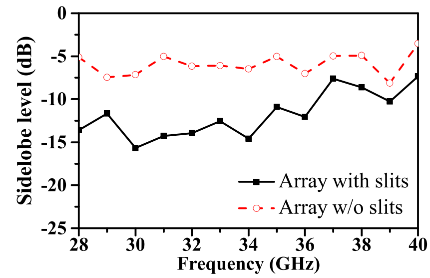

Fig. 11. Measured sidelobe levels of the horn arrays.

TABLE III
COMPARISON BETWEEN PROPOSED AND REPORTED 1×4 SUBSTRATE-INTEGRATED HORN ARRAYS

Ref.	Element Type	Element Spacing (λ_0)	Imp. BW (-10 dB)	Max. Gain (dBi)	Sidelobe Level (dB)
[5]	Dielectric loaded horn	0.9	1.5%	13.75	-10
[12]	Metamaterial loaded horn	0.98	12.5%	13.7	-12
[13]	Slot etched horn	0.96	1.4%	10.4	-12.5
This work	Dipole array loaded horn with slits	2.3	33%	14.6	-12.5

IV. CONCLUSION

A 1×4 substrate-integrated H-plane horn array with a large element spacing of $2.3\lambda_0$ has been presented. A substrate-integrated dipole array is used for widening the bandwidth and improving the radiation properties, whereas the gap SIW structures is introduced to obtain an approximately uniform field distribution over the horn aperture, which leads to the reduced sidelobe level and enhancing gain throughout a wide operating band. A fabricated prototype has demonstrated that a wide bandwidth of 33%, gain up to 14.6 dBi, and the stable radiation pattern with sidelobe level of almost less than –10 dB can be achieved. The proposed design taking advantages of a simple configuration and promising operating features is attractive for wideband millimeter-wave wireless applications.

References

[1] E. Pucci, E. Rajo-Iglesias, J.-L. Vazquez-Roy, and P.-S. Kildal, "Planar dual-mode horn array with corporate-feed network in inverted microstrip gap waveguide," *IEEE Trans. Antennas Propag.*, vol. 62, no. 7, pp. 3534–3542, Jul. 2014.

[2] T. Sehm, A. Lehto, and A. V. Räisänen, "A high-gain 58 GHz box-horn array antenna with suppressed grating lobes," *IEEE Trans. Antennas Propag.*, vol. 47, no. 7, pp. 1125–1130, Jul. 1999.

[3] Z. L. Li and K. Wu, "A new approach to integrated horn antenna," in *Proc. Int. Symp. Antenna Technol. Appl. Electromagn.*, Jul. 2004, pp. 535–538.

[4] M. E. Morote, B. Fuchs, J. F. Zurcher, and J. R. Mosig, "A printed transition for matching improvement of SIW horn antennas," *IEEE Trans. Antennas Propag.*, vol. 61, no. 4, pp. 1923–1930, Apr. 2013.

[5] H. Wang, D. G. Fang, B. Zhang, and W. Q. Che, "Dielectric loaded substrate integrated waveguide (SIW) *H*-plane horn antennas," *IEEE Trans. Antennas Propag.*, vol. 58, no. 3, pp. 640–647, Mar. 2010.

[6] M. E. Morote, B. Fuchs, J. F. Zurcher, and J. R. Mosig, "Novel thin and compact *H*-plane SIW horn antenna," *IEEE Trans. Antennas Propag.*, vol. 61, no. 6, pp. 2911–2920, Jun. 2013.

[7] Y. Zhao, Z. X. Shen, and W. Wu, "Wideband and low-profile *H*-plane ridged SIW horn antenna mounted on a large conducting plane," *IEEE Trans. Antennas Propag.*, vol. 62, no. 11, pp. 5895–5900, Nov. 2014.

[8] L. Wang, X. X. Yin, S. L. Li, H. X. Zhao, L. L. Liu, and M. Zhang, "Phase corrected substrate integrated waveguide *H*-plane horn antenna with embedded metal-via arrays," *IEEE Trans. Antennas Propag.*, vol. 62, no. 4, pp. 1854–1861, Apr. 2014.

[9] L. Wang, M. E. Morote, H. Y. Qi, X. X. Yin, and J. R. Mosig, "Phase corrected *H*-plane horn antenna in gap SIW technology," *IEEE Trans. Antennas Propag.*, vol. 65, no. 1, pp. 347–353, Jan. 2017.

[10] N. B. Makou and A. A. Kishk, "Substrate integrated horn antenna with uniform aperture distribution," *IEEE Trans. Antennas Propag.*, vol. 65, no. 2, pp. 514–520, Feb. 2017.

[11] J. Wang *et al.*, "Wideband dipole array loaded substrate integrated *H*-plane horn antenna for mllimeter waves," *IEEE Trans. Antennas Propag.*, vol. 65, no. 10, pp. 5211–5219, Oct. 2017.

[12] Y. Cai, Y. S. Zhang, L. Yang, Y. F. Cao, and Z. P. Qian, "Design of low-profile metamaterial-loaded substrate integrated waveguide horn antenna and its array applications," *IEEE Trans. Antennas Propag.*, vol. 65, no. 7, pp. 3732–3737, Jul. 2017.

[13] Y. Luo and J. Bornemann, "Substrate integrated waveguide horn antenna on thin substrate with back-lobe suppression and its application to arrays," *IEEE Antennas Wireless Propag. Lett.*, vol. 16, pp. 2622–2625, 2017.

[14] C. A. Balanis, *Antenna Theory: Analysis and Design*, 3rd ed. Hoboken, NJ, USA: Wiley, 2005.

[15] D. Deslandes and K. Wu, "Accurate modeling, wave mechanisms, and design considerations of a substrate integrated waveguide," *IEEE Trans. Microw. Theory Tech.*, vol. 54, no. 6, pp. 2516–2526, Jun. 2006.

[16] RO4000 High Frequency Laminates, Ansoft Corp., Canonsburg, PA, USA, Rogers Corp., Woodstock, CT, USA. [Online]. Available: http://www.rogerscorp.com/documents/726/acs/RO4000-LaminatesData-Sheet.pdf

[17] D. Dousset, K. Wu, and S. Claude, "Millimeter-wave broadband transition of substrate-integrated waveguide to rectangular waveguide," *Electron. Lett.*, vol. 46, no. 24, pp. 1610–1611, Nov. 2010.